Metallophysics and Advanced Technologies
Металофіз. новітні технол.
Metallofiz. Noveishie Tekhnol.
2026, vol. 48, No. 8, pp. 907–918
https://doi.org/10.15407/mfint.48.08.0907
Reprints available directly from the publisher

© 2026 G. V. Kurdyumov Institute for Metal Physics,
National Academy of Sciences of Ukraine
Published by license under
the G. V. Kurdyumov Institute for Metal Physics–
N.A.S. of Ukraine Publishers imprint.
Printed in Ukraine.

PACS numbers: 06.60.Vz, 46.50.+a, 61.72.Ff, 61.72.Hh, 62.20.M-, 81.20.-n, 81.40.Np

Influence of Ti 6Al 4V Alloy Microstructure and Processing Parameters of Hot Deformation (Forging) on the Formation of Cup-Shaped Product

O. M. Ivasyshyn, H. A. Bahlyuk*, V. I. Bondarchuk, S. F. Kyrylyuk*, and P. Ye. Markovs'kyy

G. V. Kurdyumov Institute for Metal Physics, N.A.S. of Ukraine,
36, Academician Vernadsky Blvd.,
UA-03142 Kyiv, Ukraine
**I. M. Frantsevich Institute for Problems of Materials Science, N.A.S. of Ukraine,*
3, Omeljan Pritsak Str.,
UA-03142 Kyiv, Ukraine

The influence of the microstructure type of the titanium Ti–6Al–4V alloy on the formation of a cup-shaped part by two-stage hot plastic deformation by forging is studied. As found, surface cracks in a strictly localized region form in the case of a globular $\alpha+\beta$ microstructure, whereas this is not observed in a microstructure with unrecrystallized plastic particles of the α-phase. A scheme explaining such a locking action of the α-phase plates is proposed, and performed finite-elements' simulation has established the occurrence of a complex stress state in this area, which causes the nucleation of surface cracks.

Key words: titanium, Ti–6Al–4V alloy, microstructure, hot deformation, forging, stresses.

Досліджено вплив типу мікроструктури титанового стопу Ti–6Al–4V на формування чашоподібної деталі двостадійним гарячим пластичним деформуванням куванням. Було виявлено, що у випадку ґлобулярної $\alpha+\beta$-

Corresponding author: Pavlo Yevhenovych Markovs'kyy
E-mail: pmark@imp.kiev.ua

Citation: O. M. Ivasyshyn, H. A. Bahlyuk, V. I. Bondarchuk, S. F. Kyrylyuk, and P. Ye. Markovs'kyy, Influence of Ti–6Al–4V Alloy Microstructure and Processing Parameters of Hot Deformation (Forging) on the Formation of Cup-Shaped Product, *Metallofiz. Noveishie Tekhnol.*, **48**, No. 8: 907–918 (2026). DOI: 10.15407/mfint.48.08.0907

© Publisher PH 'Akademperiodyka' of the NAS of Ukraine, 2026. This is an open access article under the CC BY-ND license (https://creativecommons.org/licenses/by-nd/4.0)

мікроструктури утворюються поверхневі тріщини у строго локалізованій області, тоді як у мікроструктурі з некристалізованими пластичними частинками α-фази цього не спостерігається. Запропоновано схему, що пояснює таку замикальну дію пластин α-фази, а проведене моделювання методом скінченних елементів встановило виникнення складного напруженого стану в цій області, що викликає зародження поверхневих тріщин.

Ключові слова: титан, стоп Ti–6Al–4V, мікроструктура, гаряче деформування, кування, напруження.

(Received 17 July, 2026; in final version, 22 July, 2026)

1. INTRODUCTION

Titanium alloys are ones of the most important structural materials for a wide range of applications due to the unique combination of their properties—high specific strength and ductility, fatigue characteristics, corrosion resistance, and non-magnetism [1–3]. In addition, these alloys are characterized by good processability; to obtain the desired properties, they are subjected to various types of deformation and heat treatment [2–4]. These treatments can be divided into treatments for the purpose of creating a certain internal phase composition and microstructure (which determines the mechanical characteristics of the material) and treatments that form a specific product. Often, the optimal parameters and modes of these two types of treatments do not coincide. For example, to obtain the considered most optimal globular (equiaxed) microstructure in titanium alloys, thermomechanical treatment with compression ratios of more than 80% is required, carried out at temperatures lower than the β-transition temperature [3, 5]. At the same time, to simplify the processes of shaping in various types of deformation (from rolling to pressing and forging) and to use effectively equipment and tools, it is desirable to carry out deformation processing at the highest possible temperatures. The latter approach critically spoils the microstructure of titanium alloys, catastrophically reducing their properties, firstly plasticity [5, 6]. At the same time, it is impossible to state unequivocally that titanium alloys have one universal microstructure for all cases and practical applications. For example, the highest strength characteristics are possessed by alloys with highly dispersed inclusions of the primary α-phase obtained by quenching from temperatures of a single β-phase field and subsequent aging [1, 7], while the resistance to crack propagation and high-temperature creep is better in a coarse-grained lamellar microstructure [1, 6, 8]. The present work is concerned with the study of the influence of the structural features of the microstructure of the Ti–6 Al–4V [wt.%] alloy on its hot deformability in the manufacture of such a relatively simple, but widely used in real practice object as a ‘cup’.

2. MATERIAL AND EXPERIMENTAL PROCEDURE

Two ∅30 mm rods (Fig. 1, *a*) of commercial Ti–6Al–4V [wt.%] alloy produced by different companies were used as initial material to produce 'cup' shaped object (Fig. 1, *b*) by means of two-step hot forging. One of these rods has bi-modal type of microstructure type consisting of primary α-globules and fine mixture of lamellae secondary α + β in all locations—in the centre and near the rod edge (Fig. 2, *a*, *b*). The second one is characterized by similar bimodal microstructure in the centre (Fig. 2, *c*), but not completely recrystallized microstructure with laminated in longitudinal direction α- and β-phases in the zone near the edge of the rod (Fig. 2, *d*).

Hot forging of the samples of the rods with both microstructures was performed in two steps. In the first step, after heating at 920°C for 30 min, the outer hemispherical shape of the forged peace was formed with a die. Moreover, in the second, the inner cavity was formed using a reverse extrusion scheme of deformation. At least 5 forged pieces were produced from each type of the rods.

The manufactured forgings were first examined over their entire surface to detect possible defects. Cracks were found on the outer surface of products made from the rod with microstructure 1, while products made from the rod with microstructure 2 had no defects. The article containing surface defects was then cut (as shown in Fig. 3) for a detailed study of the microstructure and its relationship with crack formation. Microstructural studies were performed using scanning electron microscopy (SEM, using TESCAN Vega 3 microscope) on sec-

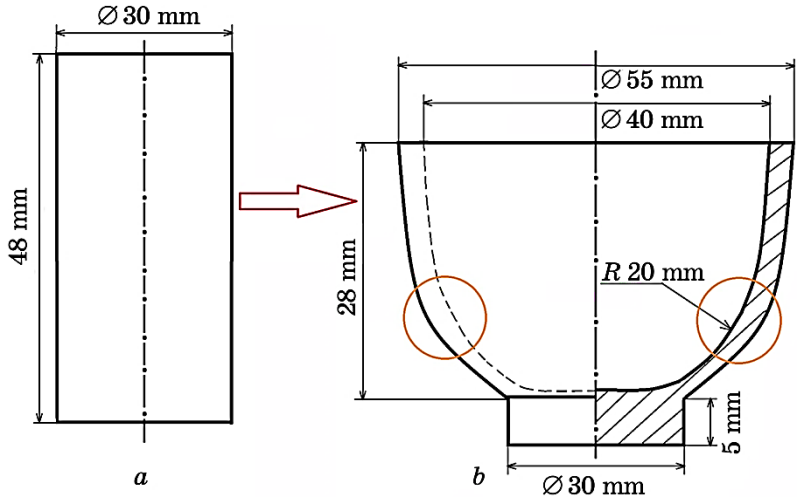


Fig. 1. Schematic presentation of the initial rod (*a*) and final shape of the forged piece (*b*).

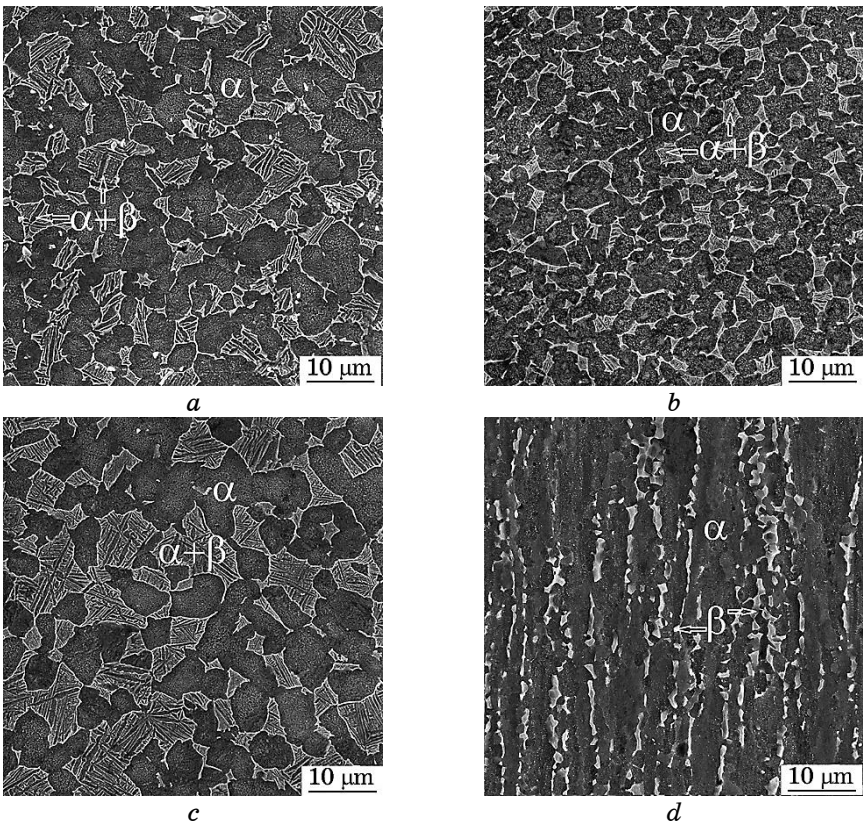


Fig. 2. Microstructure of the 1st (*a*, *b*) and the 2nd (*c*, *d*) ∅30 mm rods in the initial state in the centre (*a*, *c*) and near the edge (*b*, *d*). (SEM, SE).

tions prepared according to the standard method for this alloy in its etched with Kroll solution state [9].

To explain the influence of hot deformation conditions on the localization of stresses and deformations during the formation of forged pieces, a finite element simulation was carried out by means of the finite element method [10] using the DEFORM 2D/3D software. Based on the modelling results, the deformed state was established and the distribution of effective strain ε_i in the forging volume at various transitions was analysed:

$$\varepsilon_i = \frac{\sqrt{2}}{3}\int_0^t \sqrt{(\dot{\varepsilon}_z - \dot{\varepsilon}_r)^2 + (\dot{\varepsilon}_z - \dot{\varepsilon}_\varphi)^2 + (\dot{\varepsilon}_r - \dot{\varepsilon}_\varphi)^2 + \frac{3}{2}\dot{\gamma}_{rz}^2}\, dt\,, \tag{1}$$

$$\dot{\varepsilon}_z = \frac{\partial V_z}{\partial z},\ \dot{\varepsilon}_r = \frac{\partial V_r}{\partial r},\ \dot{\varepsilon}_\varphi = \frac{V_r}{r},\ \dot{\gamma}_{rz} = \frac{1}{2}\left(\frac{\partial V_r}{\partial z} + \frac{\partial V_z}{\partial r}\right), \tag{2}$$

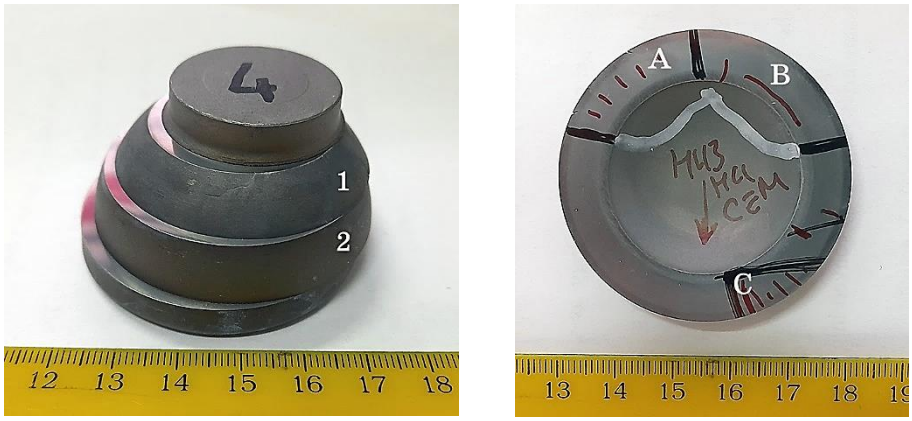
where V_r and V_z are radial and axial components of the velocity vector.

3. RESULTS AND DISCUSSION

3.1. Study of Microstructure after Hot Deformation

During the initial visual examination, cracks were found in areas (A), (B) and (C) indicated in Fig. 3, *b* and Fig. 4, *a*. In two areas marked as (A) and (C), cracks are visible, directed tangentially at an angle of approximately 45° from the outer surface into the depths of the forged peace (1–4 in Fig. 4, *a*). The presence of such cracks in the products is a fact, causing their complete rejection. All these cracks had practically the same character and appearance. Details of the microstructure of a typical crack 4 are shown in Fig. 4, *b*–*e*. In Figure 4, *b*, it can be seen that the crack extends to a depth of approximately 2 mm from the surface. At its most superficial edge (Fig. 4, *c*—locations (A) and (B) are identical), traces of plastic deformation are visible in the areas both around the crack itself (marked by arrow *1*) and at the outer surface of the forging (arrow *2*). However, in the deeper zone at the tip of the crack (Fig. 4, *c*), it is already clearly visible that it grew along a narrow channel of a highly deformed structure, which is very similar to the adiabatic shear band (ASB [11], marked with an arrow). Moreover, this ASB extends dipper into the deformed material (Fig. 4, *e*).

An adiabatic shear band is a narrow region in a material, often a metal, where intense shear deformation occurs under high strain rates, leading to a rapid temperature rise that is not dissipated to the surroundings. The formation of ASB involves complex microstructural



a *b*

Fig. 3. General view of the divisional ones of the forged pieces (*a*) and its cross-section in the layer (1), where the surface cracks were discovered (*b*).

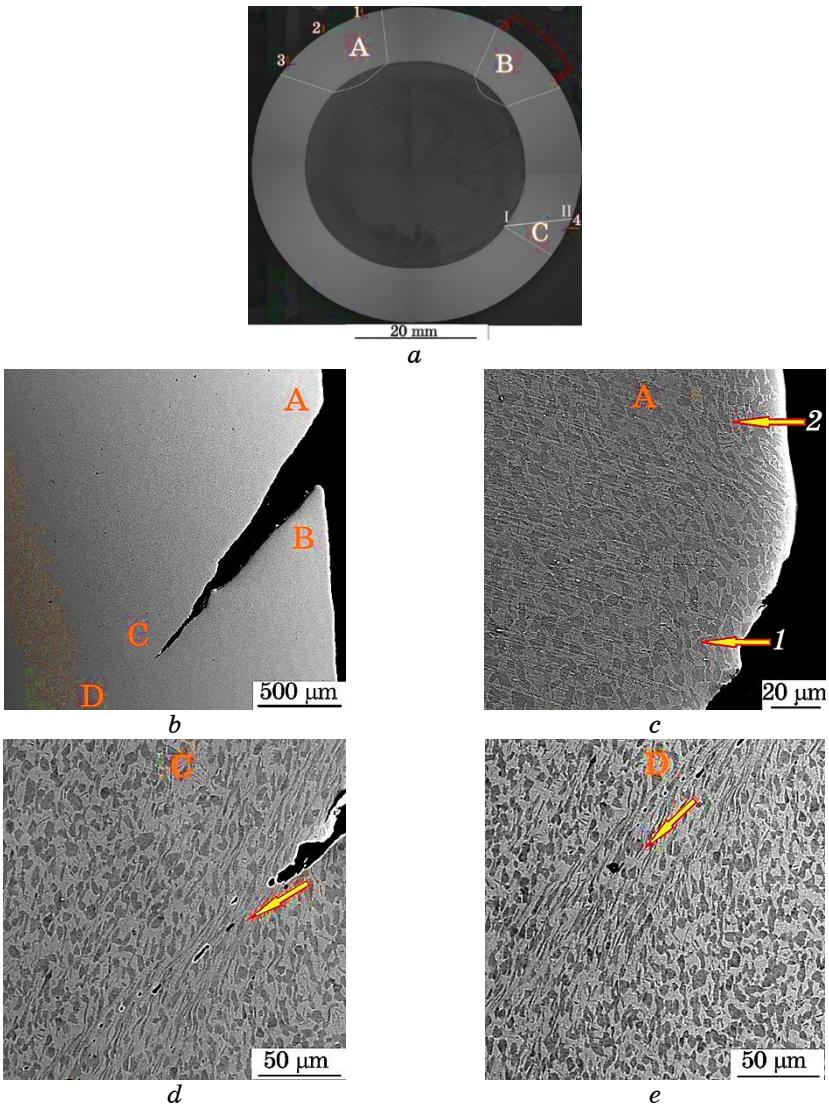


Fig. 4. General view (*a*) of section 1 (from Fig. 3, *b*), and microstructure of the crack 4 (*b*–*e*) in the different locations indicated in (*b*). Arrows in (*c*–*e*) indicate elements of microstructure discussed (SEM, BSE).

changes, such as dynamic recrystallization, which contribute to the observed material softening [11, 12].

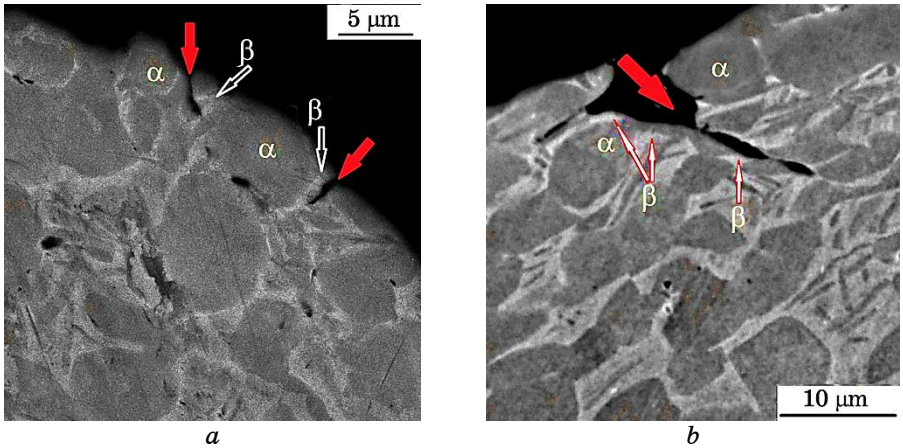
These results of microstructural studies explain the nature of the formation of such deep cracks in the microstructure of the 1st type due to the localization of deformation in certain areas of the surface with the formation of adiabatic shear bands. The special nature of such ASB

[13] leads to strong local heating of the material and its weakening, which causes cracking. Nevertheless, these results do not explain how the initial stage of the origin of such cracks occurs. In addition, this does not explain the fact that, in the microstructure of the 2nd type with a banded structure of phases in the near-surface layers, cracks do not arise.

To solve this problem, additional studies were carried out in other areas to detect smaller cracks, those at the earliest stage of crack initiation. Such cracks (Fig. 5) were found in area (B) shown in Fig. 4, *a*. In Fig. 5, *a*, *b*, it is evident that small cracks originate in the surface layer itself at the boundaries between the stronger particles of the α-phase [8] and the softer interlayers of the β-phase. Further, with increasing load, such cracks continue to spread in depth along the same 'weakened' interphase α/β boundaries. A similar phenomenon, in principle, was observed earlier, mainly in the case of the spread of fatigue cracks under alternating loading [14].

In the forged pieces obtained from rods with the second type of microstructure, no cracks were found. However, analysing the above results, one can come to a fairly well founded conclusion that even if such a microcrack can form on the surface, then, as can be seen in Fig. 2, *d*, there will be no such 'weakened' α/β-interphase boundary in front of it.

Instead, the tip of the microcrack will rest against a plate of stronger α-phase, which will lie across its path. A comparison of these situations is shown in the form of a conditional diagram in Fig. 6. It is obvious that, for the propagation of cracks deeper inside the forging body (shown in Fig. 4), the nucleation of such small cracks on the surface is



a *b*

Fig. 5. Small (initial) cracks on the surface of forgings processed with 1st microstructure rod. Red arrows indicate direction of cracks (SEM, BSE).

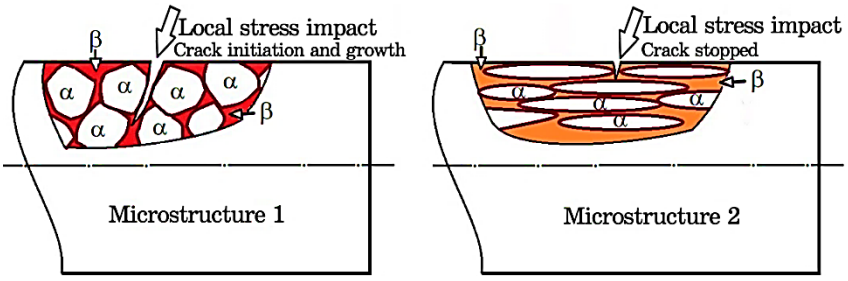


Fig. 6. Scheme illustrating influence of microstructure in the surface layers on surface cracks propagation.

a necessary condition.

3.2. Modelling of Deformation

The results of modelling the temperature fields and the deformed state of the forging volume during each of the two deformation transitions confirm the hypothesis regarding the deformation nature of the local temperature changes (Figs. 7–10). First of all, it should be noted that the deformation production of a product of this shape is carried out in two stages: first, by forming an intermediate bell-shaped product from a cylindrical blank (Fig. 7, *a*), and then by forming an internal cavity inside it (Fig. 7, *b*).

As can be seen from Fig. 7, *a*, already at the first forging operation, in which the open-die forging scheme is implemented in most of the forging volume, preheated to 920°C, deformation heating of the material occurs, which is accompanied by an increase in temperature to

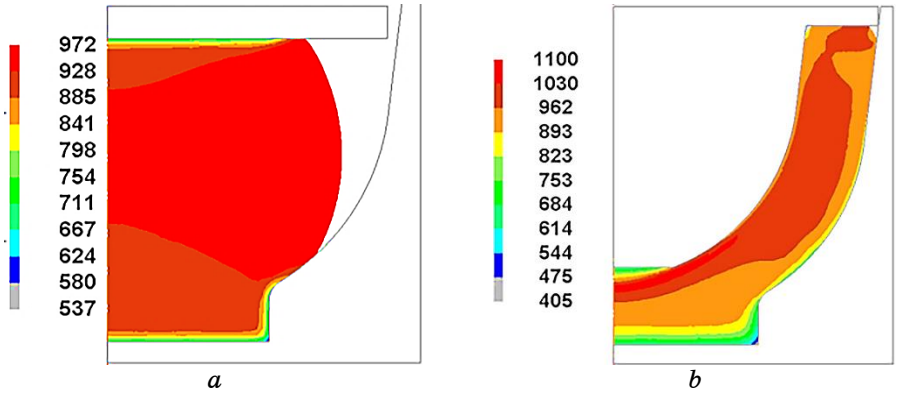


Fig. 7. Distribution of temperature fields in the forging volume after the first (*a*) and second (*b*) forging operations.

more than 970°C in local zones subjected to greater deformations.

In the second forging transition, the temperature of the lower (cylindrical) part of the forging and the peripheral layers of the spherical part of its surface, due to contact with the colder working surface of the die, decreased to 750–820°C in the cylindrical part and to 890–960°C on the lateral spherical part (Fig. 7, *b*).

The deformation nature of temperature changes in local zones of the forging is confirmed by the results of modelling the effective strain distribution across its cross-section (Fig. 8), which correlates quite closely with the nature of the temperature distribution. As can be seen in Fig. 8, *a*, the highest values of effective strain are observed in the central zone of the forging during the first pass and decrease in the radial direction towards the peripheral areas. In contrast, the lower cylindrical zone of the forging is marked by the minimum values of effective strain.

At the same time, in the peripheral region of the forging, bordering the transition zone from cylindrical to spherical surfaces, there is a narrow region of increased deformation (indicated by an arrow), directed tangentially at an angle of approximately 45° from the outer surface into the depths of the forged peace (Fig. 8, *a*). Its location and direction are similar to the area and direction of cracks in the forging, as shown in Fig. 3 and Fig. 4.

However, taking into account the fact that the effective strain is a scalar quantity, which is considered as a generalized indicator of deformations [15] to identify the causes of the cracks formation on the surface of forgings, it is obviously also necessary to have information on the distribution of radial and axial deformations over the volume of the forging at different stages of deformation. Thus, the analysis of the patterns of radial deformation fields distribution shows, that, similarly to the pattern of the effective strain, already at the first stage of

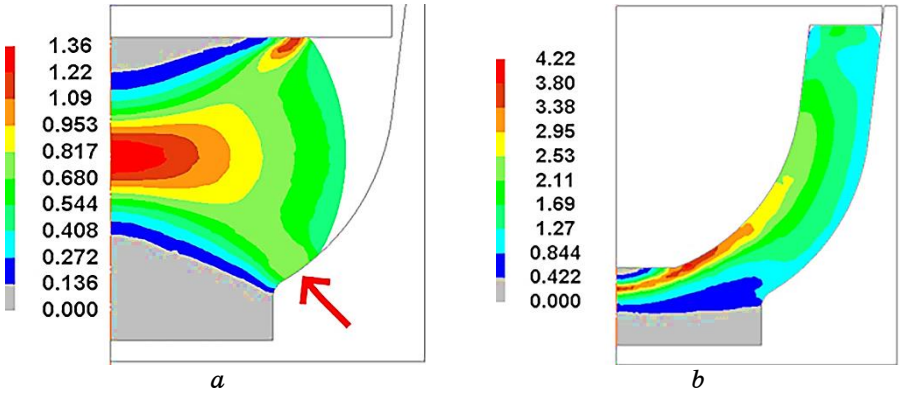


Fig. 8. Distribution of effective strain fields in the forging volume after the first (*a*) and second (*b*) forging operations.

the process in the peripheral region of the forging at the boundary of the transition from cylindrical to spherical surfaces, a narrow zone of increased level of radial deformations with a positive sign (arrow) is also formed, which corresponds to tensile deformations.

The level of the values in this zone after the first transition is in the range of 0.30–0.38 (Fig. 9, *a*); however, during the forging process at the second transition, they gradually decrease from 0.21–0.36 (Fig. 9, *b*) to a value close to zero (Fig. 9, *c*, *d*).

The noted effect of reducing the level of the values at the second transition is due to the 'wedge-forming' action of the punch when it is pressed into the forging body, at which the rate of radial deformation of local volumes located in the zone of action of the punch acquires a significantly negative value, *i.e.*, compression deformations are realized.

Obviously, the hypothesis given regarding the mechanism of crack occurrence from the point of view of the deformed state of the forging can be considered debatable referring to the significantly larger values of tensile radial deformations in the central zone of the forging (direct-

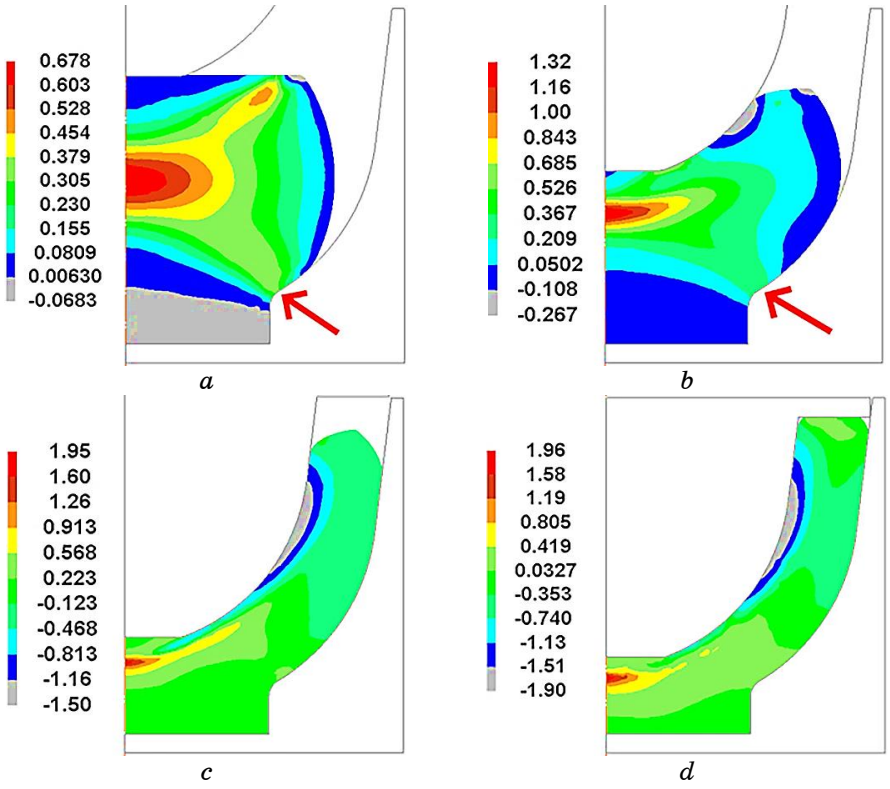


Fig. 9. Distribution of radial deformation fields in the forging volume after the first (*a*) and second (*b*–*d*) forging operations.

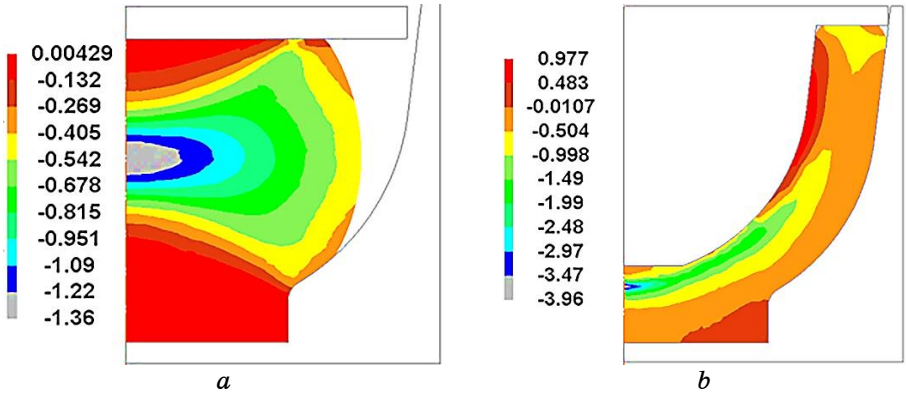


Fig. 10. Distribution of axial deformation fields in the forging volume after the first (*a*) and second (*b*) forging operations.

ly under the punch), reaching the values of 1.2–1.6 and more, in which, nevertheless, cracks are not observed. However, the assessment of the values of axial deformations ε_z under the punch shows that, in this zone, they reach negative values up to –1.5––1.9 (which indicates a significantly compressive nature of the deformations). This fully compensates for the tensile radial deformations and makes it impossible for the material to crack in this zone.

In contrast, the value of ε_z on the side surface of the forging in the area of crack formation, although it has a negative value (of about –0.011) (Fig. 10), approaches zero in magnitude, which in no way can compensate for significant tensile deformations.

4. CONCLUSION

Thus, the results of the microstructure study clearly demonstrated that the formation of surface cracks in a strictly localized region occurs in the case of the initial alloy microstructure of the globular type, which was previously considered the best in terms of mechanical properties. However, in contrast to this, the microstructure with incompletely globularized phases showed no such cracking. Based on a detailed study of the microstructure of surface layers and the nature of the initiation and propagation of such cracks in them, a scheme was proposed that shows the inhibitory effect of lamellar particles of the stronger α-phase on the growth of a such surface cracks.

To explain the somewhat unexpected location of formation of such cracks, a finite element simulation of such hot deformation was carried out. Based on the obtained data, a hypothesis is proposed regarding the mechanism of crack formation on the side surface of the forg-

ing from the point of view of their deformed state. It is based on the formation of noticeable tensile deformations in this zone during the forging process, while local axial deformations approach zero in magnitude, which in no way compensates for tensile deformations.

Part of this work was performed in G. V. Kurdyumov Institute for Metal Physics, N.A.S. of Ukraine within the framework of the project 060/23 funded by the National Academy of Sciences of Ukraine.

AUTHORS' CONTRIBUTIONS

O. M. Ivasyshyn provided general guidance for the research, set tasks, discussed the results, and participated in writing the article, H. A. Bahlyuk analysed the modelling results and prepared their description for publication, V. I. Bondarchuk performed microstructural investigations, S. F. Kyrylyuk performed computer modelling of hot deformation processes for titanium alloy and prepared graphic materials for further analysis, P. E. Markovs'kyy performed structural experiments, summarized the results of experimental studies and modelling, wrote the draft of the article and participated in its final revision.

REFERENCES

1. G. Lütjering and J. C. Williams, *Titanium* (2nd ed.) (Berlin–Heidelberg–New York: Springer: 2007).
2. M. Peters, J. Kumpfert, C. H. Ward, and C. Leyens, *Adv. Eng. Mater.*, **5**, No. 6: 419 (2003).
3. M. Niinomi, *Metall. Mater. Trans. A*, **33**: 477 (2002).
4. T. L. Jones, K. Kondoh, T. Mimoto, N. Nakanishi, and J. Umeda, *Key Eng. Mater.*, **551**: 118 (2013).
5. P. E. Markovsky, *Metallofiz. Noveishie Tekhnol.*, **31**, No. 4: 511 (2009) (in Russian).
6. S. L. Semiatin, *Metall. Mater. Trans. A*, **51**: 2593 (2020).
7. O. M. Ivasishin, P. E. Markovsky, S. L. Semiatin, and C. H. Ward, *Mat. Sci. Eng. A*, **405**, Nos. 1–2: 296 (2005).
8. P. E. Markovsky and S. L. Semiatin, *Mater. Sci. Eng. A*, **528**, Nos. 7–8: 3079 (2011).
9. https://www.struers.com/en/Knowledge/Materials/Titanium
10. Sh. Kobayashi, S.-I. Oh, and T. Altan, *Metal Forming and the Finite-Element Method* (New York–Oxford: Oxford University Press: 1989).
11. S. P. Timothy, *Acta Metall.*, **35**, No. 2: 301 (1987).
12. P. E. Markovsky, J. Janiszewski, D. G. Savvakin, O. O. Stasiuk, K. Cieplak, P. Baranowski, and S. V. Prikhodko, *Materials and Design*, **223**: 111205 (2022).
13. Y. Guo, Q. Ruan, S. Zhu, Q. Wei, J. Lu, B. Hu, X. Wu, and Y. Li, *J. Mech. Phys. Solids*, **135**: 103811 (2020).
14. G. Lütjering, *Mater. Sci. Eng. A*, **243**, Nos. 1–2: 32 (1998).
15. V. M. Danchenko, V. O. Hrynkevich, and O. M. Golovko, *Teoriya Protsesiv Obrobky Metaliv Tyskom* [Theory of Processes of Metal Working by Pressure] (Dnipropetrovsk: Porogi: 2008) (in Ukrainian).